A 6-YEAR PROSPECTIVE STUDY OF 620 STRESS-DIVERSION SURFACE (SDS) DENTAL IMPLANTS

Gary R. O'Brien, DDS
Aron Gonshor, PhD, DDS
Alan Balfour, BSBE

KEY WORDS

Clinical trial
Dental implants
Resorbable blast medium
Finite element analysis
Stress-diversion surface
Isodensity radiography

A 6-year prospective study was conducted to assess the clinical success rates and crestal bone response of a dental implant system with a stress-diversion design. Mathematical modeling, digital radiography with applied isodensity, and finite element analysis were used to highlight the effect of the stress distribution design. A total of 386 hydroxyapatite-coated prototypes and 234 commercial grit-blasted external hex implants were placed in virgin bone as well as various grafted maxillary regions, with 36% of the posterior implants being immediately loaded. Prototypes achieved 96.6% survival over a 3-year period. The grit-blasted implant, placed from 2000 to 2003, showed a 95% survival rate. There were no significant changes in crestal bone levels after the first 12 months of prosthetic loading. Engineering evaluations suggested that undesirable stresses were distributed from the crest of the ridge down through the center of the implant body.

INTRODUCTION

The physiologic response of crestal bone levels surrounding an osseointegrated implant can be separated into 3 general phases.

The first phase is associated with primary site preparation and has been well documented in the literature.[1] Crestal bone loss during the first phase has been attributed to poor surgical technique, inadequate quality and quantity of bone, or a preexisting osseous defect not previously controlled.[2,3]

The second phase would be described as the uncovering phase. Crestal bone loss associated with this surgical phase is scarcely reported in the literature due to the noninvasive nature of the procedure.

The third phase is that of prosthetic loading and function. Crestal bone loss in this phase is multifactorial and well reported in the literature.[4–6] These ''ailing and failing'' implants have introduced a new discipline within the field of implant dentistry, attempting to reverse or repair the obvious clinical problems of crestal bone loss.[7,8] Reports of excessive crestal bone loss have

Gary R. O'Brien, DDS, *is in general practice in Los Angeles. Address correspondence to Dr O'Brien, 411 North Central, Suite 225, Glendale, CA 91203 (e-mail: drobrien@scidentistry.com).*

Aron Gonshor, PhD, DDS, *is in private practice and is a lecturer at McGill University, Oral and Maxillofacial Surgery, Montreal, Quebec, Canada.*

Alan Balfour, BSBE, *is an independent biomedical engineering consultant who assisted in the design of the SDS Dental Implant, and is located in Petaluma, California.*

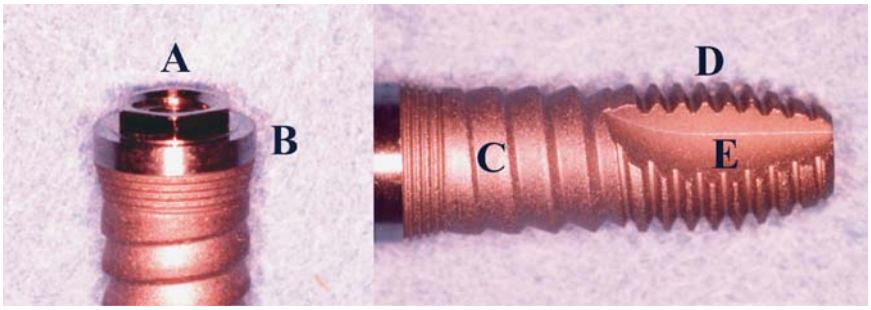

FIGURE 1. The study implant: (A) standard external hex, (B) polished 0.7-mm titanium collar, (C) 6.5-mm with stress-diversion thread, (D) tapered self-tapping implant body, (E) cutout in the driving thread.

been suggested to be a result of plaque-induced peri-implantitis[9] or occlusal overload, the latter producing excessive stresses in the crestal bone surrounding the implant.[10,11] Publications demonstrating bone loss at the crestal ridge of implants associated with microbial infections noted that it occurred only after occlusal overload.[12,13] One study, utilizing a primate model, demonstrated that occlusal overload was more responsible for crestal bone loss than plaque accumulation by more than a threefold difference.[14] Both photoelastic and finite element analysis (FEA) demonstrate that the highest concentration of stress at the implant/bone interface occurs within the area of crestal bone.[15–17] High crestal implant-to-bone stresses may also accelerate the accumulation of plaque in a similar way that occlusal stresses increase plaque accumulation around natural dentition.[18] The increased threshold to tactile perception, associated with up to 50 times greater force in dental implants, subjects the dental implant to the increased risk of occlusal overload.[19,20] Desmodontal structures refer to all physical, chemical, and physiological structures associated with the myriad of events within the dental and periodontal attachment apparatus. This system is a complex sympathetic and parasympathetic coordination of all neuromuscular structures of the myofacial system, designed to prevent overload and harmful assaults to the natural dentition.[21] This is missing in the peri-implant region due to the missing desmodontal structures.[22,23] Their absence in dental implants enhances harmful stresses and puts dental implants at greater risk for crestal bone loss than natural teeth.[24,25] Late failure of osseointegrated dental implants is most commonly the result of bone loss at the crest of the alveolar ridge.[26] The clinical reality of this ever-present problem in implant dentistry has led to a myriad of solutions.

In recent years, studies have focused on improving the clinical success of osseointegrated implants by evaluating the effect of design and shape.[27–29] Bioengineering has played a major role, with its increasing effectiveness in determining the optimum design for implant configuration and the prosthetic superstructure.[30–32] Geometric analysis of the dental implant has shown a threaded architecture to be a more favorable design for ideal stress distribution, when compared with nonthreaded implants.[33] Mathematical and mechanical modeling of the bone surrounding an implant can provide theoretical information concerning the effects of implant geometry and the bone environment.

There is an ideal envelope of stress that encourages a physiologic osteoblast response in bone remodeling and a corresponding relative magnitude of stress associated with the process of bone resorption and maturation.[34] However, it has yet to be scientifically and clinically proven which thread configuration would be most favorable in evenly distributing the stress of occlusion. The objective of this prospective study is to clinically analyze the effectiveness of a dental implant with a stress-diversion design in minimizing crestal bone loss and enhancing bone maturation below the bone crest.

METHOD AND MATERIALS

The SDS implant (Stress Diversion Surface, ACE Surgical, Brockton, Mass), shown in Figure 1, is made of type IV commercially pure titanium. This surface is treated with a resorbable blast medium (RBM).[35] All prosthetic connections are the industry standard external hex (Figure 1A). The transition from the prosthetic connection to the thread configuration is characterized by a highly polished 0.7-mm titanium surface (Figure 1B). The coronal, or proximal 6.5 mm of the thread (Figure 1C), is the stress-diversion thread configuration. It consists of 1 continuous thread that progressively changes the thread angle and inner minor diameter while holding the major diameter constant. This thread is mathematically designed to divert the stress of occlusal load away from the crest of the ridge and into the

implant body. The thread transitions into a continuous self-tapping tapered design.

Tables 1 and 2 demonstrate the distribution of implant placement in bone after surgical placement. At least 70% were placed in the first 2 years of the study. The majority of the implants were 15 mm in length (64.1%), with the 13- and 10-mm lengths representing 19.6% and 16.3%, respectively, of all implants placed. The largest numbers of implants (138, or 59%) were loaded immediately, while 96 (41%) were unloaded. There was some variability in the depth to which the head of the implant was placed relative to the crest of the ridge. In 158 implants (67.5%), the top of the implant neck was crestal, while 76 (32.4%) were up to 1 to 1.5 mm above the crest.

A minority of the implants (91, or 38.8%) was placed into native bone with no additional grafting, while the remainder were placed with the addition of some type of augmentation material: (1) an amino acid peptide and anorganic bone mineral (PepGen P-15, Dentsply Ceramed Dental, Lakewood, Colo) alone, (2) a combination of this anorganic bone mineral and deproteinated mineralized cancellous bone allograft (Puros, Zimmer Dental, Carslbad, Calif), (3) an allograft mixture with autologous platelet rich plasma (PRP), or (4) subantral augmentations with a combination of PRP with a freeze-dried demineralized bone allograft, deproteinated human cortical bone (banked tissue), and a microfibrillar bovine collagen hemostatic agent (Collastat OBP, Integra Corp, Plainsboro, NJ) (Table 2). Implants were placed in all jaw locations with the anterior and posterior mandible, as well as the anterior maxilla, each containing close to 50 implants. A larger number, or 92 (39%), were placed in the posterior maxilla. Of these 92 implants, 51 (22%) were placed in a subantral augmentation. It is also noteworthy that 36% of these posterior implants were immediately loaded.

TABLE 1
SDS implants placed per 6-mo time period after start of study

	Time (months)						
	0–6	6–12	12–18	18–24	24–30	30–36	Total
No. of implants	58	27	14	82	53	0	234

Each implant in the study was documented radiographically and positioned by means of a standard Rinn Kit, with an assigned isodensity value of 4. Digital reverse polarization techniques were used to evaluate the qualitative changes in the surrounding bone. Within a given digital radiograph, using constants (the implant body), the relative changes to the surrounding tissues were compared and analyzed by means of the Vix-Win computer program.[36,37] In the present program, the same number of pixels/mm^2 represents an area of "isodensity," and given the color yellow.[38] Every area with the same density will show the same color, based on the degree of mineralization. Figure 3 is an example of this type of analysis. Figure 3A shows the digital radiograph of 2 study implants in the lower left first molar position. This radiograph was taken 18 months after insertion of the implants and 12 months after occlusal loading. The bitmap format of the digital radiographs allow for standardization of sequential radiographs over the duration of the study. Note also the isodensity mapping of similar areas on the adjacent teeth. Figure 3B is the same radiograph with isodensity mapping of a different region of the bone surrounding the implant. Figure 3 also shows a comparable isodensity mapping for a conventional screw-type implant, depicting the crest of the ridge (C) and the remainder of the implant body (D) after 2 years in function.

Mechanical modeling of implant geometry and bone environment made use of the modeling technique known as finite element analysis (FEA) and was accomplished by using the Ansys 5.3 software program (Ansys Corporate, Canonsburg, Pa), a commercially available FEA code (G.R.O., unpublished data).[39]

RESULTS

There were a total of 620 implants placed over a 6-year period (Figure 2). From 1997 to 2000, a prototype design was used. This implant was coated with hydroxyapatite, and was machined without the continuous helical thread configuration, while still maintaining varying angles of incidence. Out of the 386 prototypes placed, 13 (3.4%) have been removed due to total implant failure. Four of these 13 implants were removed within the first month due to extremely poor quality of bone. Five of the failing implants were removed due to postsurgical infection related to immediate extraction. The remaining implants were removed as a consequence of premature overload associated with immediate placement and habitual grinding. The remaining implants

TABLE 2
Number of SDS implants in various grafting procedures*

	Virgin Bone		Allografts			
	No grafting	PepGen	PepGen + Puros	PRP	PRP + FDDB + DHCB + Colostat (in subantral augmentation)	Total
No. of implants	91	45	7	46	45	234

*PepGen P-15 is amino acid peptide and anorganic bone mineral; Puros, mineralized cancellous bone allograft; PRP, platelet-rich plasma; FDDB, freeze-dried demineralized human cortical bone (50–100 μ); DHCB, deproteinated human cortical bone; Collastat OBP, microfibrillar bovine collagen hemostatic agent (0.3 g/5 cm^3).

demonstrated consistent bone maintenance and associated circumferential maturation, as opposed to crestal bone loss. In the surviving 96.6% of the implants, there were no signs of crestal wear.

The 234 implants placed in the years 2000–2003 (Figure 2) were the current commercial design, with an RBM surface treatment. Twelve of these implants were removed. Eight of the 12 failed due to prosthetic overload at the time of immediate placement. Four of the 8 failures were in a subantral augmentation of 1 patient. The failures in this case can be attributed to patient neglect and heavy bruxism. Two failures were implants placed in immediate extraction sites with pre-existing chronic endodontic infections. The remaining 2 implants were removed due to overload at the time of immediate placement. Three of the 12 failures were in the area of the right lower molars. These implants were prematurely exposed and in very poor quality bone. The failure sites have been grafted with the intent of replacing the removed implants.

Of the 222 implants remaining, 11 (4.4%) had 1 to 2 mm of horizontal bone loss after the first 6 months of prosthetic loading. An additional 6 showed similar bone loss after 12 months. There was no change in the radiographic appearance or probing in these implants in the following recall visits. Those implants that showed bone loss were associated with the group of 91 (Table 2) that were placed in virgin osteotomies. This might suggest that the bone loss was due to surgical trauma and not prosthetic overload. They also fell into the category of the 76 implants where the head of the implant was placed above the crest of the ridge. Poor initial osseous contouring or quality of bone would most likely explain this bone-loss pattern. It is noteworthy that there were no significant changes in the bone level after 12 months of prosthetic loading.

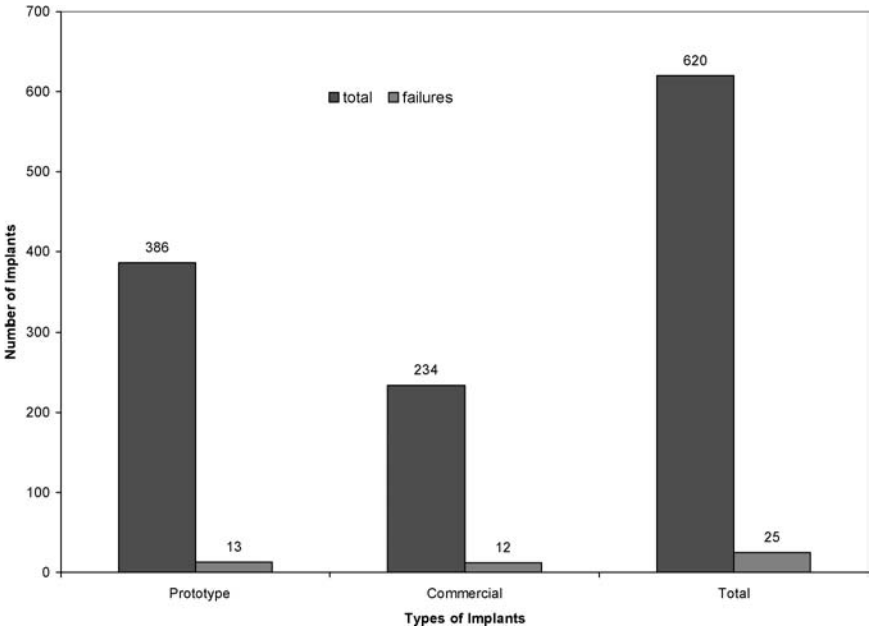

FIGURE 2. Number of failures in the 6-year implant study.

The 3-dimensional FEA of the study implant design, when compared with the industry standard Branemark (Nobel Biocare, Yorba Linda, Calif) screw implant design, clearly demonstrate that simulated occlusal loads were more evenly distributed in the first 6 to 8 mm of the study implant, with diversion of the stress from the crest of the ridge down into the implant body. Figure 4A shows the FEA of a 13-mm study implant (left) and a 13-mm standard implant (right). The surrounding bone matrix was

assigned a modulus of elasticity of 8 GPa (gigapascals) to replicate cortical bone. An on-axis compression load of 50 pounds of force (average occlusal load) was introduced with equal parameters in both models. Crestal stress was reduced to 579 pounds per square inch (PSI), depicted by the smaller red band (maximum von Mises stress) around the study implant at the crest of the ridge. The medium stress bands in green on the study implant depict an increase in stress distribution. That is, stress is diverted away from the crest of the ridge and is redirected 2 to 8 mm below the crest, in even bands, by the implant's thread configuration. The standard implant does not demonstrate this same pattern, as evidenced by the absence of medium (green) stress bands in the center of the implant body as well as the increased presence of yellow and red stress band at its crestal region. In fact, the increased maximum von Misses stress band (red) over the 1- to 2-mm coronal area of the implant has a value of 859 PSI, which is a 48% greater stress application to this area when compared with the study design. Figure 4B depicts 13-mm study (left) and standard (right) implants. The surrounding bone matrix was again assigned a modulus of elasticity of 8 Gpa. A transverse cantilever load of 4.535 inch-pounds, which generates significantly higher application stress, was also introduced with equal parameters to both models. These transverse loads were generated by applying a compressive load of 14.4 pounds 8 mm from the central axis of the implant. Again, Figure 4B depicts the highest red stress band (maximum von Mises stress of 8058 PSI) at the crest of the ridge for the standard implant. The corresponding FEA plot of the study implant, with the same parameters, again shows the minimized crestal red band (maximum von Mises stress of 5626 PSI) and a more even distribution of stress, depicted by the increased blue bands at the implant's thread configuration. Under these transverse loading conditions, the standard implant's maximum crestal stress was found to be 43% higher than the study implant's thread design, which correlates with the on-axis compressive loading results.

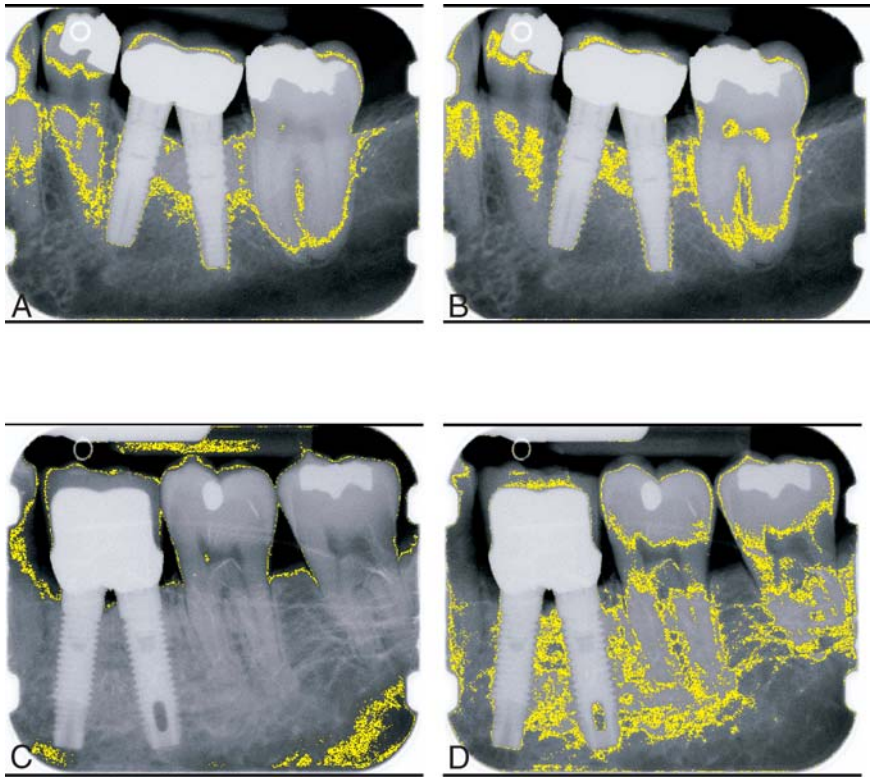

FIGURE 3. Isodensity marking on bone around the (A) study implant configuration at the crest of the ridge and other regions of equal density, (B) at the study implant thread portion of the implant, (C) at the crest of the ridge of a standard screw implant, and (D) the remainder of the standard implant body.

DISCUSSION

Once an implant is integrated, prosthetic loading introduces forces to the implant-bone interface and the surrounding connective tissue strata, which are directed through the implant and into the surrounding supportive anatomy. The implant body and its physical properties remain a constant. The supportive anatomy surrounding the dental implant is an everchanging, visco-elastic medium of multipotential cells, with the unique ability to change form and structure to accommodate the desired task. This unique collection of connective tissue will be referred to as the peri-implant substrate. The more rigid the connection between the superstructure and this peri-implant substrate, the more force-absorbing demand is placed on the implant and its surroundings.

The laws and principles associated with the science of biomechanical engineering govern all aspects of the load dynamics and stress distribution associated

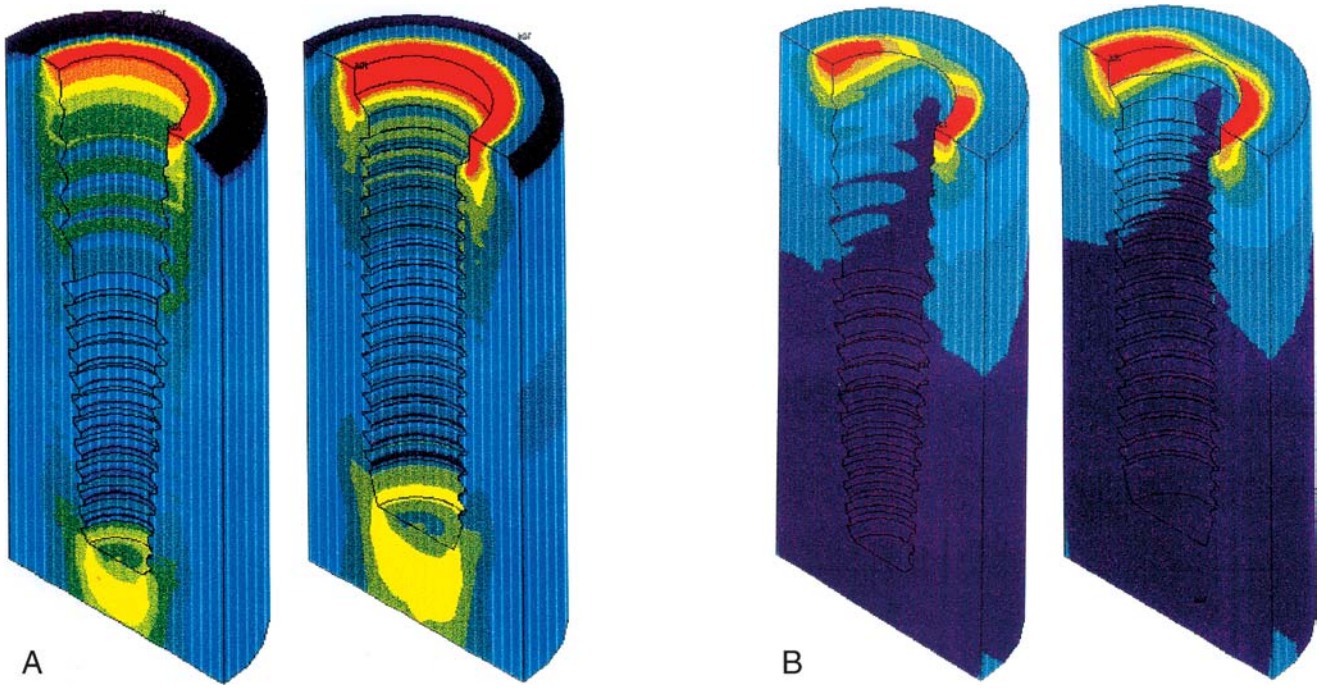

FIGURE 4. Finite element analyses of the study implant and standard screw-type implants showing von Mises stresses. In both pairs of schematics, the study implant is on the left and the standard screw implant is on the right. (A) Depicts on-axis compressive loading of 50 pounds of force (average occlusal load) with equal parameters in both models. Note the reduction in crestal stress, depicted by the smaller red band (maximum von Mises stress) around the study implant at the crest of the ridge versus the standard design. (B) Depicts these same implants under off-axis transverse cantilever loading of 4.535 inch-pounds. Again, the study implant shows a decrease in the crestal stress (red) band and the dispersion of these stresses toward the center of the implant.

with the forces of occlusion and the distribution of those forces. Material science has given us a clear and predictable mathematical explanation of the constants within our prosthetic system. The peri-implant substrate presents with an infinite range of densities, volumes, and modulus of elasticity. This variation also changes with each patient and even with each site in the oral cavity. We are able to establish some ranges in the areas of modulus of elasticity, density, and the percent of surface area contact, but these remain variables when mathematically describing the stress distribution around a dental implant. The isodensity mapping of bone surrounding the stress-diversion design implants demonstrates a maintenance of a crestal attachment at the very top of the implant after a year in function (Figure 3A) as well as an increased region of bone maturation associated with the stress-diversion thread portion of this implant (Figure 3B). This increase in density suggests distribution of stress away from the crest of the ridge to a more favorable location 2 to 8 mm below the crest. The mapping of a standard screw-type implant, in Figure 3C, shows the maintenance of a crestal attachment, with similar bone density at the top of the implant. Figure 3D demonstrates the isodensity mapping of an indiscriminate medullary pattern of bone after 2 years of occlusal loading. Although there is no sign of crestal saucerization or bone loss, there is also no sign of positive maturation of bone related to functional load as seen in the stress-diversion implant design.

Finite element analysis (FEA) has demonstrated that the nature of the connection, as well as the properties of the surrounding bone, greatly influence stress distribution.[37] Several studies have demonstrated that implant geometry and diameter create both positive and negative influences on stress distribution.[40] The study dental implant was conceived with the intention of evenly distributing the stresses of occlusion away from the crest of the ridge.

When a prosthesis is put into function, the forces associated with the load dynamics are distributed through the rigid connections and into the surrounding connective tissue. These forces seek out the most rigid material and connection to aid in the support necessary for the particular function. There is material fatigue and component breakage, if given enough time and force to allow this form of damage. In certain cases, bone

degeneration often starts at the most rigid connection closest to the origination of the load. Mathematically, it can be demonstrated that the compressive forces introduced by an occlusal load can be up to 5 times greater than the corresponding tensile forces.[40] It would stand to reason then that to reduce the harmful stresses at the crest of the ridge, one would be encouraged to convert these stresses from compressive to tensile.[40] Looking at the mathematical derivation of stress analysis within changing thread values, the ideal angle of incidence and surface area can be extrapolated as

$$\Delta \sum \chi = \Delta \sum \gamma(\tfrac{1}{2} \sin \alpha), \quad (1)$$

where $\Delta\sum \chi$ is the change in the forces introduced in the surrounding bone, and $\Delta \sum \gamma$ is the change in the sum of the forces of occlusion. One can see that, as the angle of incidence (sin α) or the pitch of the thread is increased, the corresponding transverse force into the bone ($\Delta\sum \chi$) is decreased.

Using this formula, the angles necessary to maximize tension at the crest and minimize compression can be derived. The distance stress must travel down the body of the implant also counterbalances further stress distribution. This leads to a more even force distribution throughout the first 6 to 8 mm. This inherently would help compensate for the increased stresses associated with implant dentistry. This stress distribution would also be more likely to yield values within that ideal zone associated with bone development and maturation.[41] The FEA samples indicate a reduction of both maximum stresses and/or collar region stresses for various osseous models. This stress distribution indicates that, in carrying loads, the study implant uses more of the surrounding bone material than does the standard screw implant. One can see that the combination of high stresses in the collar region, from both compression and bending, can cause resorption and bone loss in this region, leading to "saucerization." Therefore, the study implant, through proper clinical use, could aid in the reduction of these stresses and resulting bone loss. For there to be a total of only 17 implants with postprosthetic crestal bone changes, given the wide range of clinical applications, is of clinical relevance. This would present a total of 91.7% of the remaining implants, over the given time period, with no sign of crestal degeneration associated with prosthetic loading.

In more evenly distributing the load, within the envelope of ideal stress for proper bone maturation,[34] the study implant design may help to encourage greater bone maturation. Reiger et al[42] have suggested that often an implant's design not only creates maximum stress at the neck and apex but transfers relatively low stresses to the bone along the body of the implant. This leads to bone loss in the middle of the implant due to atrophy, while at the same time causing bone loss at the extremities due to excessive stress. In this study, there have been no significant radiographic signs of postprosthetic crestal saucerization, often seen in other designs within the first 1 to 2 years of prosthetic loading.[43,44]

CONCLUSION

The study implant with a change in conventional thread configuration achieved a 96% survival rate, with placement in all areas of the jaws, in both grafted and virgin bone, with up to 3 years of functional loading. Finite element analysis and isodensity radiographic mapping suggest that the stress-diversion thread design may lead to more evenly distributed load.

REFERENCES

1. Adell R, Lekholm U, Rockler B. A 15-year study of osseointegrated implants in the treatment of the endentulous jaw. *J Oral Surg.* 1981;10:387–416.

2. Friberg B, Jemt T, Lekholm U. Early failures in 4,641 consecutively placed Branemark dental implants: a study from stage 1 surgery to the connection of completed prostheses. *Int J Oral Maxillofac Implants.* 1991;6:142–146.

3. Jaffin RA, Berman CL. The excessive loss of Branemark fixtures in type IV bone: a 5-year analysis. *J Periodontol.* 1991;62:2–4.

4. Mombelli A, van Oosten MAC, Schurch E, et al. The microbiota associated with successful or failing osseointegrated titanium implants. *Oral Microbial Immunol.* 1987;2:145–151.

5. Rosenberg ES, Torosian JP, Slots J. Microbial differences in 2 clinically distinct types of failures of osseointegrated implants. *Clin Oral Implants Res.* 1991;2:135–144.

6. Misch CE. Density of bone: effect on treatment plans, surgical approach, healing, and progressive bone loading. *Int J Oral Implantol.* 1990;6:23–31.

7. Lozada JL, James RA, Boskovic M, et al. Surgical repair of peri-implant defects. *J Oral Implantol.* 1990;16:42–46.

8. Meffert RM. How to treat ailing and failing implants. *Implant Dent.* 1992;1:25–33.

9. Albrektsson T, Isidor F. Consensus report of session IV (implant dentistry). In: Lang NP, Karring T, eds. *Proceedings of the First European Workshop on Periodontology.* Chicago, Ill: Quintessence; 1994:365–369.

10. Isidor F. Loss of osseointegration caused by occlusal overload of oral implants: a clinical and radiographic study in monkeys. *Clin Oral Implants Res.* 1996;7:143–152.

11. Quirynen M, Naert I, van Steenberghe D. Fixture design and overload influence marginal bone loss and fixture success in the Branemark system. *Clin Oral Implants Res.* 1992;3:104–111.

12. Lekholm U, Adell R, Branemark P-1. Complications. In: Branemark P-1,

Zarb GA, Albrektsson T. *Tissue-Integrated Prostheses. Osseointegration in Clinical Dentistry.* Chicago, Ill: Quintessence Publishing; 1985:233–240.

13. Spray JR, Black CG, Morris HF, et al. The influence of bone thickness on facial marginal bone response: stage 1 placement through stage 2 uncovering. *Ann Periodontol.* 2000;5:119–128.

14. Isidor F. Loss of osseointegration caused by occlusal overload of oral implants: a clinical and radiographic study in monkeys. *Clin Oral Implants Res.* 1996;7:143–152.

15. Deines DN, Eick JD, Cobb CM, et al. Photoelastic stress analysis of natural teeth and three osseointegrated implant designs. *Int J Periodontics Restorative Dent.* 1993;13:540–549.

16. Widera GEO, Tesk JA, Privitzer E. Interaction effects among cortical bone, cancellous bone, and periodontal membrane of natural teeth and implants. *J Biomed Mater Res Symp.* 1976;7:613–623.

17. Ko CC, Kohn DH, Hollister SJ. Micromechanics of implant/tissue interfaces. *J Oral Implantol.* 1992;18:220–230.

18. Glickman I, Smulow JB. Effect of excessive occlusal forces upon the pathway of gingival inflammation in humans. *J Periodontol.* 1965;36:144–147.

19. Hammerle CH, Wagner D, Bragger U, et al. Threshold of tactile sensitivity perceived with dental endosseous implants and natural teeth. *Clin Oral Implants Res.* 1995;6:83–90.

20. Jacobs R, van Steenberghe D. Comparison between implant-supported prostheses and teeth regarding passive threshold level. *Int J Oral Maxillofac Implants.* 1993;8:549–554.

21. Lundgren D, Laurell L. Occlusal force pattern during chewing and biting in dentitions restored with fixed bridges of cross-arch extension. I. Bilateral end abutments. *J Oral Rehabil.* 1986;13:57–71.

22. Lundgren D, Laurell L. Occlusal force pattern during chewing and biting in dentitions restored with fixed bridges of cross arch extension. II. Unilateral posterior two-unit cantilevers. *J Oral Rehabil.* 1986;13:191–203.

23. Falk H, Laurell L, Lundgren D. Occlusal interferences and cantilever joint stress in implant-supported prostheses occluding with complete dentures. *Int J Oral Maxillofac Implants.* 1990;5:70–77.

24. Isidor F. Histological evaluation of periimplant bone at implants subjected to occlusal overload or plaque accumulation. *Clin Oral Implants Res.* 1997;8:1–9.

25. Isidor F. Loss of osseointegration caused by occlusal overload of oral implants: a clinical and radiographic study in monkeys. *Clin Oral Implants Res.* 1996;7:143–152.

26. Parr GR, Steflik DE, Sisk AL, et al. Clinical and histological observations of failed two stage titanium alloy basket implants. *Int J Oral Maxillofac Implants.* 1988;3:49–55.

27. Hoshaw SJ, Brunski JB, Cochran GVB. Mechanical loading of Branemark implants affects interfacial bone modeling and remodeling. *Int J Oral Maxillofac Implants.* 1994;9:345–360.

28. Quirynen M, Naert I, Steenberghe D. Fixture design and overload influence marginal bone loss and implant success in the Branemark system. *Clin Oral Implants Res.* 1992;3:104–111.

29. Teixeira ER, Sato Y, Akagawa Y, et al. A comparative evaluation of mandibular finite element models with different lengths and elements for implant biomechanics. *J Oral Rehabil.* 1998;25:299–303.

30. Masuda T, Yliheikkila PK, Felton DA, et al. Generalizations regarding the process and phenomenon of osseointegration. Part I. In-vivo studies. *Int J Oral Maxillofac Implants.* 1998;13:17–29.

31. Hoshaw SJ, Brunski JB, Cochran GVB. Mechanical loading of Branemark implants affects interfacial bone modeling and remodeling. *Int J Oral Maxillofac Implants.* 1994;9:345–360.

32. Quirynen M, Naert I, Steenberghe D. Fixture design and overload influence marginal bone loss and implant success in the Branemark system. *Clin Oral Implants Res.* 1992;3:104–111.

33. Siegele D, Soltesz D. Numerical investigations of the influence of implant shape on stress distribution on the jaw bone. *Int J Oral Maxillofac Implants.* 1990;4:333–340.

34. Urist MR, ed. *Fundamental and Clinical Bone Physiology.* Philadelphia, Pa: JB Lippincott; 1980:160–162.

35. BioCoat, Inc. *Technical Data on the RBM Surface Roughening Treatment.* Southfield, Mich: BioCoat, Inc; 1996.

36. Firebaugh MW. Computer graphics. Tools for visualization. Dubuque, Iowa: WmC Brown Publishers; 1993.

37. Kay DC, Levine JR. *Graphics File Formats.* 2nd ed. New York, NY: Windcrest/McGraw-Hill Inc; 1995.

38. Accusoft Corporation Image Gear. *Dentopix Digital Imaging System.* Des Plaines, Ill: Gendex Dentsply Int; 1996–2002.

39. Clift SE, Fisher J, Watson CJ. Finite element stress and strain analysis of the bone surrounding a dental implant: Effect of variations in bone modulus. *Proc Inst Mech Eng [H].* 1992;4: 233–241.

40. Akca K, Iplikcioglu H. Evaluation of the effect of the residual bone angulation on implant-supported fixed prosthesis in mandibular posterior edentulism Part II: 3-D finite element stress analysis. *Implant Den.* 2001; 4:238.

41. Huiskes R, Numaker D. Local stresses and bone adaptation around orthopaedic implants. *Calcif Tissue Int.* 1984;36:S110–S117.

42. Reiger MR, Mayberry M, Brose MO, Finite element analysis of six endosseous implants. *J Prosthet Dent.* 1990;63:671–676.

43. Misch CE. Density of bone: effect on treatment plans, surgical approach, healing, and progressive bone loading. *Int J Oral Implantol.* 1990;6:23–31.

44. Rosenberg ES, Torosian JP, Slots J. Microbial differences in 2 clinically distinct types of failures of osseointegrated implants. *Clin Oral Implants Res.* 1991;2:135–144.